

FUSION OF DEEP LEARNING AND HANDCRAFTED FEATURES FOR MELANOMA DETECTION

Misbah Javed

Department of Computer Science, The Superior University, Lahore, 54000, Pakistan
misbahjaved911@gmail.com

Aneeqa Javed

Department of Pharmacy Lahore Leads University, Lahore, 54000, Pakistan

Amina Javed

Department of Computer Science, The Punjab University, Lahore, 54000, Pakistan

Muhammad Azam

Department of Computer Science, The Superior University, Lahore, 54000, Pakistan

Muhammad Mahtab

Department of Computer Science, The Superior University, Lahore, 54000, Pakistan

Abstract:

Melanoma is resulting in high numbers of fatalities in humans, and is regarded as being one of the most aggressive and dangerous forms of skin cancer. Early diagnosis must be made to maximize the chances of survival, but scalability, precision, and interpretability of the machine and human diagnostic approaches currently being utilized are constrained. This paper offers a hybrid method that merges deep learning features derived using the InceptionV3 convolutional neural network with handcrafted ones like "Color Histograms" and "Histogram of Oriented Gradients (HOG)". A "Support Vector Machine (SVM)" is employed for classification once a fusion technique unifies the complementary strengths of the two types of features. The model is evaluated using the "ISIC2019 Skin Cancer HAM10000" dataset. The 98% accuracy of the proposed method demonstrates the efficacy of concatenating handcrafted features with deep learning for strong melanoma diagnosis. With its solution to key issues in automated skin lesion analysis with a sound and interpretable framework, this paper showcases a set of opportunities for effective clinical application.

Introduction

Individuals all over the world are battling from different types of cancers (Zainab et al., 2025). But among all the cancers discovered until now, skin cancer numbers to be most lethal and therefore is very fatal, leading to many deaths among individuals all over the globe. Ensemble deep learning methods have shown promise in improving the accuracy of skin cancer detection (Sardar et al., 2024). Its development is primarily due to long exposure to the damaging ultraviolet (UV) radiation from the sun that results in mutations of the DNA of skin cells, thus leads to uncontrollable cellular proliferation. Amongst all the cancers, skin cancer is placed on the fifth rank based on its occurrence in the world (Nasim & Ahmad, 2025). Scary forecasts show that in the near future, cancer will outstrip cardiovascular diseases as the major cause of mortality for individuals and a big barrier to the enhancement of life expectancy across the world. The International Agency for Research on Cancer (IARC) states that in 2018, a total of over 18.1 million new cancer cases and 9.6 million cancer-related deaths cases globally were reported (Garner et al., 2023). Under this vast category, skin cancer continues to make a substantial contribution to the cancer burden worldwide. The American Cancer Society indicates that melanoma is the most advanced type of skin cancer affecting about 6% of all new cancers in men and 4% in women in 2023. Additionally, it is projected that the incidence of new melanoma will keep increasing within the next two decades because of heightened UV exposure, population growth, and environmental influences. Though melanoma is said to occur in a minor percentage—less than 1%—of total cases of skin cancer, yet it accounts for the majority of deaths due to skin cancer, due to its virulent metastatic nature and lack of response to treatment at later stages.

There are primarily three forms of skin cancers "basal cell carcinoma (BCC)", "squamous cell carcinoma (SCC)", and "melanoma". The most frequent of all SCCs, BCC accounts for about 80% of all cases and 20% of all deaths due to SCC. While SCC also develops fairly slowly, it has a greater potential to invade deeper into skin layers and metastasize to other organs. Melanoma arises from melanocytes, cells that are responsible for producing pigments and are located in the basal layer of the epidermis. While melanoma cancer is the most dangerous and cause of death owing to its potential for spreading throughout the lymphatic system and blood. The American Cancer Society reports that an estimated 110,213 new cases and 7,560 deaths related to melanoma are anticipated in the United States alone in the year 2024. Melanoma's prognosis is highly dependent upon the stage at detection. If diagnosed early, the five-year survival rate is around nearly 100%; However, this drops to 66% when cancer has spread to close adjacent lymph nodes and reaches 27% if distant organs are affected.

The reason for conducting this study is the growing incidence and death rate related to melanoma. It is reported by "WHO" which said that out of every three cases of cancer report made worldwide, one is skin cancer. Melanoma was among the leading three cancers with the fastest increase in incidence during the period from 2006 to 2016, most notably in affluent nations. The rate increased by 39% over the decade, during which melanoma increased more quickly than a number of other typical cancers like thyroid or endometrial cancer. Though there has been an improvement in the diagnostic results with advances in medical imaging and dermoscopic examination, a high rate of discrimination between melanoma and non-melanoma lesions still presents a problem for most dermatologists and pathologists.

A non-invasive imaging method, dermoscopy is utilized extensively in clinical practice to analyze skin lesions. Dermoscopy offers magnified views of skin structures and aids dermatologists in detecting malignancies at the initial stages. But to perform dermoscopic diagnosis correctly, it needs physicians' expertise. Research indicates that dermoscopy alone has an accuracy rate ranging from 65% to 75% (Nami et al., 2012). Consequently, many patients end up undergoing invasive biopsies, which are not only psychologically stressful but also contribute to unnecessary healthcare spending and utilization of resources. Elmore et al. also noted the inter-observer variability among dermatopathologists during the interpretation of skin biopsy specimens, which questions consistency in diagnosis and patient outcomes.

To overcome these limitations, "Artificial Intelligence (AI)" (Zainab et al., 2025) and "Machine Learning (ML)" (Asim et al., 2025) techniques have emerged as promising tools in the medical imaging domain. Specifically, "deep learning"—a subfield of AI—has demonstrated superior performance in various medical classification tasks, including skin lesion detection, by automatically extracting high-level features from raw image data. Still, deep learning alone is not always the best solution, particularly when training sets are small or fine-grained detail in lesion characteristics is paramount for good classification (Khan et al., 2025).

There is increasingly a body of research favoring blending "deep learning features with handcrafted features" like "color histograms", shape descriptors, and texture patterns to improve model interpretability (Nasim et al., 2025) and performance (Zainab et al., 2025). Handcrafted features are extracted based on domain expertise and have conventionally been applied in traditional machine learning pipelines (Nasim et al., 2023). By the combination of handcrafted features with deep learning features learned from convolutional neural networks (CNNs), the combination method enhance strength of both methods, resulting in better accuracy, reduced false positives, and more stable performance on various datasets (Khan, 2025). This work provides a compact research for melanoma detection based on the benefits of "deep learning features, handcrafted features, and metadata-based information.". The architecture that is proposed is dependent on various different stages: segmentation of lesions

into binary classes, deep feature extraction via a pre-trained deep learning network (InceptionV3), feature extraction is performed on the basis of handcrafted features like "Histogram of Oriented Gradients (HOG)" and "Color Histograms", and both the methodologies are combined together for the final classification. Comprehensive experiments are performed to analyze the contribution of different feature types and find the optimal combination for strong melanoma detection.

The goal of this research is not just to create a high-performing model but to also evaluate the effectiveness of feature-level fusion towards improved classification accuracy. By evaluating the performance of models based on deep learning independently, handcrafted features independently, and the combined technique, we hope to give an insight into the possible advantages of hybrid modeling techniques towards detecting skin cancer.

The main goals of this study are:

- To develop and test a hybrid melanoma classification model that combines deep learning and handcrafted features.
- To determine the most discriminative features—both deep learning and handcrafted ones—that play a major role in melanoma classification accuracy.
- To conduct ablation studies between different feature fusion methods and analyze their effect on performance measures.

This research aims to answer the following question:

In what way does the combination of deep learning methods and handcrafted features impact the accuracy of melanoma identification relative to individual use of either method?

Literature Review:

The size of the biological and medical datasets is always on the rise (Zainab et al., 2025). Machine learning and artificial intelligence algorithms are now globally acclaimed for interpreting such huge and complex data (Khan et al., 2025). In particular, machine learning and deep learning tools and techniques act as supporting hand in image data analysis (Shamshirband et al., 2021). Many researchers used a diversity of approaches, including dermatology photographs of the skin, to identify melanoma skin cancer. Categorizing and identifying skin cancer with a deep neural network takes much nerves, it is claimed.

Various approaches have been used by many studies for detecting melanoma skin cancer. Artificial neural networks with multiple hidden layers emulating the design of the human brain are employed in deep learning algorithms (Khan et al., 2024). Deep learning methods provide outcomes based on data, weights, and biases (Arif et al., 2024). The term 'deep' literally implies two or more hidden layers (Tariq et al., 2025). Deep learning is applied most commonly to fields such as Computer vision (Zainab et al., 2025), object detection (Arif et al., 2023), Computer security (Khan et al., 2025), Social Engineering (Khan et al., 2024), and bioinformatics. Deep learning algorithms contain an enormous ability to extract features automatically, understand unstructured input information like text or images, and predict outcomes, that is why they are employed so frequently. So-called feature hierarchy is an important component of Deep Neural Networks (DNN).

Every hidden level of layers' trains with a certain type of feature, such as the hands, using position and hand-detecting images. Suppose, for instance, that we want to cluster together images of various types of animals such as cats, pandas and lions. Deep learning models can identify subtle but significant features such as edges, corners, boundaries and nodes in such a case, and then use those features to identify eyes, noses, mouths, and ears at a higher level. At the most sophisticated level, these features are ultimately combined to create cognitively beneficial and meaningful representations in order to predict. We call this situation forward propagation. Further, by utilizing the gradient descent algorithm and the process of back propagation, it computes prediction errors to update weights and bias and enhance prediction

accuracy (Tselios, 2022). However, there are more complex deep learning models with different topologies that have been developed to tackle certain problems based on the need. Some popular models of deep learning include Convolutional neural networks (CNN) and recurrent neural networks (RNN). The former is primarily used for image classification and computer vision tasks.

They can spot particular patterns and characteristics in images. The second type, a sequential model, is normally used on sequential data points and is mainly utilized in time series analysis and speech recognition. (Jojoa Acosta et al., 2021) shines the light on significant topic that is early detection of melanoma by suggesting a two-stage deep learning-based method consisting of Mask R-CNN for lesion segmentation and ResNet-152 for classification. With the ISBI 2017 dataset, the model obtains significant accuracy increments (3.66%) and balanced accuracy gains (9.96%) over existing benchmarks, with high sensitivity and specificity (>0.8). Dual-stage architecture guarantees strong lesion detection and discrimination between benign and malignant cases.

Although promising, the review of the literature could also compare its performance to other comparable approaches, comment on the limits of the datasets, and discuss generalizability to actual clinical situations and heterogeneous populations. (Jain & Pise, 2015) described a novel approach to identify melanoma skin cancer in several early studies. For getting a high-quality image, the skin lesion is well preprocessed and utilized for further processing. They also used edge detection and thresholding algorithms for segmentation. An overview of cyber threats generated by AI has been explored in a recent study (Arif et al., 2024). AI techniques for threat detection in cybersecurity have also been reviewed (Khan et al., 2024).

They applied technique of geometry-based features and ABCD (Asymmetry, Border, Color, and Diameter) features to feature extraction from segmented image. He grouped the images into two categories, first class was images of melanoma skin cancer and second class of images of normal skin on the basis of these extracted features. Support Vector Machines (SVM) were subsequently applied by Alquran (Rejeesh, 2019) in order to differentiate between normal skin images and cancer skin images. Preprocessing techniques were employed on the medical images prior to the development of this model. Original features were first extracted using the gray level co-occurrence matrix, PCA methods were employed to choose the individual features. They calculated the complete dermoscopy score using a "support vector machine" classification. (Adegun & Viriri, 2019) conducted a thorough work to classify between the skin lesions as normal or cancer cells. They eliminated issues, including fuzzy borders and inhomogeneity to attain efficiency. To optimize the performance of them of system they employed enhanced encoder-decoder network with skip routes. The model that was suggested was challenged on the ISBI 2017 and PH2 datasets, which yielded very impressive experiments with accuracy (95%) and dice metrics (92–93%), outclassing the conventional methods.

This research study of (Almaraz-Damian et al., 2020) integrates deep learning characteristics by employing a Mutual Information (MI) method with handcrafted features by employing a method of ABCD rule to engineer a new Computer-Aided Detection (CAD) technique to detect and classify melanoma.

The method involves a systematic way: CNN-based deep features and handcrafted feature extraction method is employed that extracts the shape, color, and texture feature, MI fusion combines the most relevant information from both the features, and preprocessing enhances and segments images of lesions. Classification involves methods like Relevant Vector Machines (RVMs), Support Vector Machines (SVMs), and Linear Regression (LR). When tested on ISIC 2018 dataset, the outcomes were highly persuasive on sensitivity, specificity, and accuracy. Significantly, it presents a new method to calibrate measurement metrics in imbalanced datasets, thus resolving an overarching problem in skin lesion classification.

| | Acc. Train | Acc. Test | Sensibility | Specificity | Precision | F-Score | AUC | G-Mean | IBA | MCC |
|--------------|--------------|--------------|--------------|-------------|--------------|--------------|--------------|-------------|-------------|---------------|
| VGG16 | 88.60 | 84.90 | 79.23 | 0.85 | 88.74 | 83.71 | 84.79 | 0.85 | 0.72 | 0.7012 |
| VGG19 | 90.23 | 87.14 | 82.46 | 0.87 | 90.44 | 86.26 | 87.05 | 0.87 | 0.76 | 0.7451 |
| Mobilenet v1 | 91.48 | 89.32 | 84.04 | 0.89 | 93.49 | 88.51 | 89.21 | 0.89 | 0.79 | 0.7898 |
| Mobilenet v2 | 92.40 | 89.71 | 86.41 | 0.90 | 92.08 | 89.16 | 89.64 | 0.90 | 0.80 | 0.7953 |
| ResNET-50 | 90.67 | 87.86 | 81.24 | 0.88 | 93.09 | 86.76 | 87.72 | 0.87 | 0.77 | 0.7624 |
| DenseNET-201 | 91.10 | 88.54 | 83.25 | 0.88 | 92.61 | 87.68 | 88.44 | 0.88 | 0.78 | 0.5985 |
| Inception V3 | 91.33 | 88.10 | 84.87 | 0.88 | 90.59 | 87.42 | 88.02 | 0.88 | 0.77 | 0.7632 |
| Xception | 90.47 | 87.53 | 83.19 | 0.87 | 90.58 | 86.73 | 87.44 | 0.87 | 0.76 | 0.7525 |

Table 1: Performance results of the proposed method using selected deep learning architectures fused by (Almaraz-Damian et al., 2020)

The ability of Computer-Aided Diagnosis (CAD) systems to minimize human effort while maintaining high classification accuracy in skin cancer identification is emphasized in the research study by (Filali et al. (2020)). It critically analyzes the advantages and limitations of machine learning (ML) and deep learning (DL) in skin lesion classification, noting that ML is capable with small datasets whereas DL is better for large datasets. To overcome each module's limitation individually, the proposed hybrid approach combines manually crafted features (e.g., shape, color, texture) with features borrowed from advanced DL models. While feature engineering is employed to improve efficiency, the phase is not highly distinctive either. Comparative study and verification on many different sets of data indicate promising results.(Filali et al., 2020)

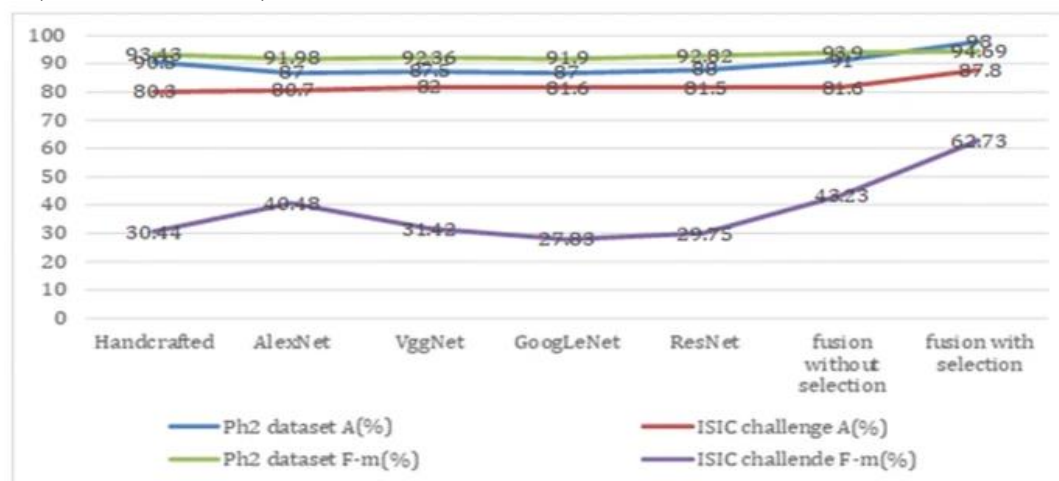


Figure 1: Outcome of the classification for both dataset using the F-measure, kappa and Accuracy by (Filali et al., 2020).

For melanoma detection in dermoscopic images, concerns like noise (hair, air bubbles) are discussed in the research by (Bansal et al., 2022). The authors propose a hybrid feature extraction technique involving handmade (HC) and deep learning models (DLMs) like ResNet50V2 and EfficientNet-B0 with three morphological processes for hair removal. Artificial Neural Network (ANN) is used for classification. The proposed approach performs better than the use of only HC or DLM features with accuracy rates of 94.9% and 98%, respectively, on the HAM10000 and PH2 dataset. The research does not discuss scalability, computational expense, and robustness of the methods on different datasets despite the positive results.

The contributions of the research in melanoma detection work would be strengthened by further comparison with state-of-the-art approaches and more detailed discussion of the hair removal method's limitations.

Benign or cancerous tumors may arise from skin cancer, which results from abnormal cell growth of the skin. Traditional diagnosis methods such as biopsies and imaging require a great

deal of time and effort. While they often lag behind in early detection, especially on unseen data, automated methods based on handcrafted feature extraction have been proposed to address this. This work led to an effective feature-fusion-based approach that can be used as a trustworthy source for skin cancer detection model. The model employs Inception V3 and Local Binary Patterns (LBP) to determine the features from images after pre-processing them through a GF filter to remove noise. An LSTM network classifies the merged characteristics as malignant or benign after an Adam optimizer adjusts the learning rate.

When it was tested on the Dermoscopy ISIC 000-image dataset, the model's accuracy, precision, and recall were 99.4%, 98.7%, and 98.66%, respectively (Mahum & Aladhadh, 2022). In another study by (Esteva et al., 2017) proposed a pre-trained model that consisted of Inception V3 and CNN, for the skin cancer classification. They achieved a 72% accuracy in the classification of the images after classifying 3374 dermoscopic images and 129,450 clinical skin cancer images. To solve this, (Jayapriya & Jacob, 2020) came up with a deep convolutional neural network-based architecture later on. Using the top classifying result of 88.92%, they implemented a Fully Convolutional Residual Network (FCRN) for real skin coup segmentation from the ISBI challenge dataset, giving 50 layers for melanoma cancer classification. (Rahman et al., 2022) work is centered on the pressing challenge of automated skin cancer identification and classification from plain dermoscopic images, with poor contrast and lesion similarity in mind. A CNN-inception-based VGG19 model is utilized for feature fusion and classification, coupled with a hybrid feature extractor (HOG, LBP, SURF) and anisotropic diffusion filtering to extract noise. With 99.85% accuracy, 91.65% sensitivity, and 95.70% specificity, the process has potential over prior conventional approaches. A cost-effective study on skin lesion detection by computer with the help of handmade and deep learning algorithms was presented by Pathan et al. (Pathan et al., 2018).

Recent studies have shown that the integration of handmade and deep learning algorithms is capable of diagnosing skin cancer effectively (Majtner et al., 2016). These are achieved through the combination of hand-designed features and deep learning techniques. As the two methods are expected to have different error profiles, we believe that this combination has the capability to yield more accurate results than either one in isolation. The traditional image processing models used in this study are image processing algorithms used to detect medically significant features, such as abnormal pigment networks (APN) and small arteries, as well as lesion color distribution patterns, which are all detected using handcrafted features (Mishra & Celebi, 2016). Data sent to the pathologist, including the patient's name, age, gender, location and size of the lesion, and family history as well as other documents specific to the melanoma, is comprised in the demographic module. The DL network is made up of a converted, pre-trained deep learning (DL) architecture refocused for classification of melanoma. To obtain deep features from images, (Hagerty et al., 2019) designed a fusion strategy that utilizes a transfer learning mechanism of ResNET-50 Convolutional Neural Network (CNN) architecture.

It is not apparent, however, what parts of their process are constituted by handmade elements. Additionally, they applied a feature selection method—in this example the 2 method—to performance revision on two data sets, one of which is an adaptation of the ISIC 2018 dataset (Codella et al., 2019).

Diagnosis of melanoma poses a number of challenges in addition to opportunity. High interclass character similarity levels only make it harder. We noticed that the pre-trained models were superior to machine learning approaches, indicating promising results. The ensemble of the individual performance of several neural networks rather than a conventional single network tries to optimize the goodness of each network result and generates remarkable predictions. Also, choosing the most effective evaluation metric for unbalanced data seems to have its effect on the research in the domain. They are often misleading if chosen improperly.

In order to supply the best representations of skin lesions towards their classification, I combined handcrafted features and deep learning models. The weighted ensemble strategic strategy was employed so that numerous multi-input models were combined to fulfill the classification task. To ensure the uniqueness of the model, the architecture was trained and tested on publicly available standard data sets. Moreover, it has been compared with the latest models in the literature. Despite the difficulties, this model performed admirably.

Research Methodology:

Dataset Description:

Dataset used for current research is ISIC2019SkinCancer HAM10000. It contains total 10000 images. From which 9600 images are used to train the model and 1000 images to test the model. Dataset includes images of skin cancer melanoma that are segregated into test and train dataset. Each of which is segregated into benign and malignant. Actinic keratosis, basal cell carcinoma, dermatofibroma, nevus, pigmented benign keratosis, seborrheic keratosis, squamous cell carcinoma, and vascular lesions all fall under the category of non-melanoma images. These categories are also divided into test and train.

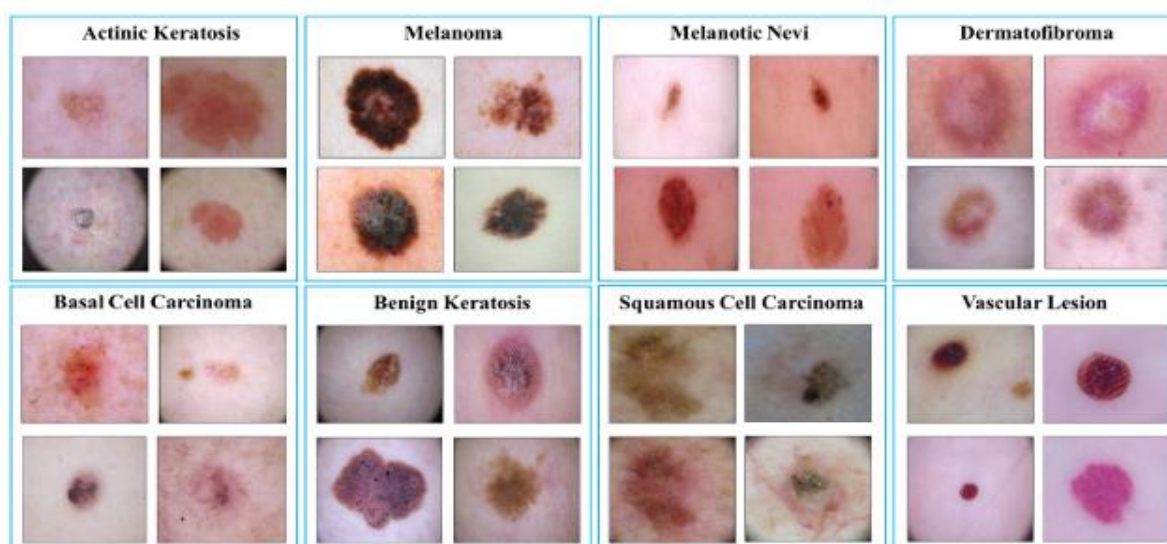


Figure 2: Skin cancer images

Methodology:

Pre-processing:

All the images in the ISIC 2018 dataset are labeled as training and testing sets. Both the sets of images exist with three-dimensional (3D) pixel values (red, green, and blue). These color images are converted to Grayscale images that is they are converted from 3D pixel values to 1D values in order to reduce the computational complexity.

Feature Extraction:

Handcrafted features

HOG features are a symbolized description of the image constructed using block patterns and cells. For each pixel, they contain information on luminosity densities according to equation 2 and shape orientations according to equation 1. Most notably, we can observe how the shape changes with each orientation.

1) As shown in equation 1, the gradient calculations of each pixel are aggregated to form a HOG features vector.

2) Employing gradient values to obtain a histogram for each block.

3) Selecting the histograms' normalization, as shown in equation 2.

Gathering the normalization vectors collectively per block(Mohammed & Melhum, 2020).

$$\text{gradient magnitude } (g) = \sqrt{g_x^2 + g_y^2}$$

$$\text{gradient magnitude } (g) = \arctan \frac{g_y}{g_x}$$

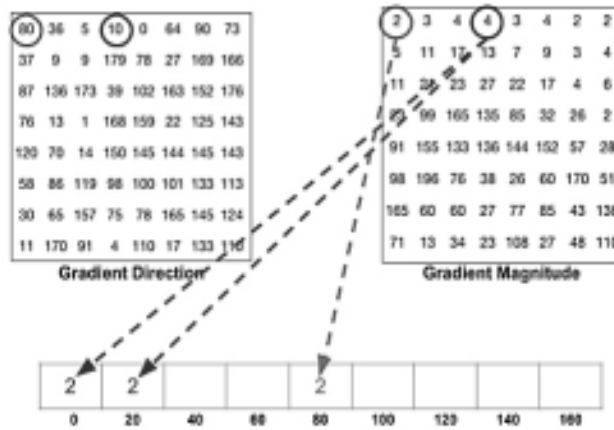


Figure 3: HOG feature extraction

Color Histogram:

A common handcrafted color descriptor for describing an image's overall global color distribution is a color histogram. It provides a statistical representation of the frequency with which different combinations of colors or intensities occur in an image. Color histograms are an excellent example of handcrafted features because they are manually constructed based on human-defined color spaces and binning mechanisms, as opposed to deep learning-based features that are automatically extracted from large datasets. The ability of color histograms to extract important visual features such as pigmentation and color variability—which are often indicative of melanoma—is the main motivating factor for their application in skin lesion analysis. Benign lesions have more regular appearances, while malignant lesions generally exhibit varying color distributions, such as deeper or multiple hues.

Its numerical representation is expressed as follows:

$$h_b = \sum_{p=1}^N \delta(B(C(p)) = b), \quad \text{for } b = 1, 2, \dots, B$$

Deep learning Features

Feature Extraction using Convolutional Neural Network

Convolutional neural networks (CNNs), which are a type of deep neural networks, were introduced successfully for the first time by LeCun in 1998 (LeCun et al., 1988). They often perform better than traditional artificial neural networks in numerous computer aided activities such as particular object detection and image classification. CNNs learn features and make predictions regarding image classes by applying input images to a series of hidden layers, such as convolutional, pooling, and fully connected.

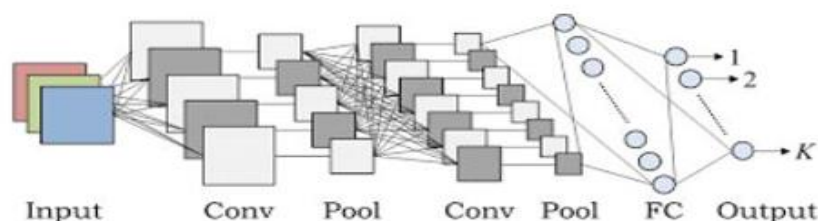


Figure 4: :Convolution neural network(Hidaka & Kurita, 2017)

The process of convolution and an activation function are typically the two main components in every convolutional neural network (CNN) model level. By using an optimized kernel to the input, a feature map is generated by the convolution layer. It is followed by a non-linear activation function, which is more commonly referred to as ReLU, and helps extract non-linear patterns by letting positive values pass unchanged and output zero for negative values. The mathematical expression of this process is

$$y_k = f(W_k * x)$$

Here, f is the activation function and W_k are weights. The dimensionality of feature maps is then reduced by pooling layers. Max pooling is a method which selects the maximum value with most prominent features and reduces computational expense, and average pooling, which computes the average of input regions, are two widely used pooling methods.

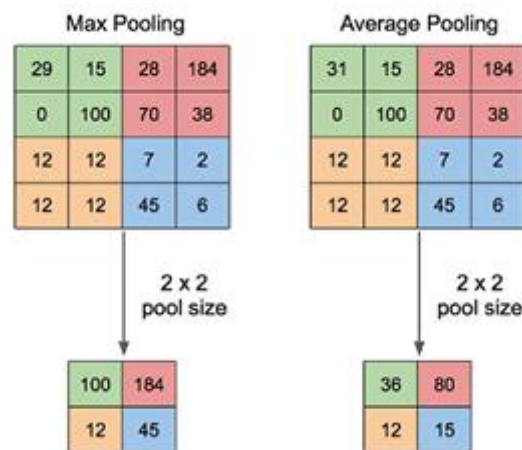


Figure 5: Picture of Max Pooling and Average Pooling (Muhamad Yani, 2019)

Feature extraction in InceptionV3:

The InceptionV3 structure, developed by Google and pre-trained on ImageNet, is employed in this research for extracting deep features (Chaturvedi et al., 2020). We can employ various kernel sizes (1×1 , 3×3 , and 5×5) simultaneously, InceptionV3 therefore enhances CNN performance and allows multi-scale feature learning. To enhance computational cost savings, the architecture decomposes larger convolutions (such as 3×3) into smaller ones (such as 1×3 and 3×1). InceptionV3 employs grid sizes of 8×8 , 17×17 , and 35×35 for spatial feature extraction, with the input resized to 299×299 pixels. Mathematical expression is given by:

$$y_k = f(W_k * x)$$

Where x is the input, W_k is the filter, and f is a non-linear activation function, $y_k = f(W_k * x)$. The definition of the ReLU activation is:

$$f(x) = \max\left[\frac{f_0}{f_0 + 1}, 0, x\right]$$

$$f(x) = \max(0, x)$$

For training, gradient computation uses the chain rule of calculus. The derivative is as follows if $i \in R$ is a scalar function of vector $j \in R$:

$$\frac{\partial i}{\partial j} = [\frac{\partial i}{\partial j_1}, \frac{\partial i}{\partial j_2}, \dots, \frac{\partial i}{\partial j_h}]$$

$$\frac{\partial j}{\partial i} = [\frac{\partial j}{\partial i_1}, \frac{\partial j}{\partial i_2}, \dots, \frac{\partial j}{\partial i_h}]$$

$$\frac{\partial i}{\partial j_1}, \frac{\partial i}{\partial j_2}, \dots, \frac{\partial i}{\partial j_h}$$

$$j_1, j_2, \dots, j_h$$

$[\partial i]$

The following is the definition of the cross-entropy loss function used for classification:

$$L = -\sum_{l=1}^L t(l) \log q(l)$$

where $q(l)$ is the anticipated likelihood and $t(l)$ is the true label. The following is how label smoothing is used to handle label overconfidence:

$$p'(t|k) = (1 - \epsilon)\delta_{l,k} + \epsilon L$$

$$\text{For } t|k, p' = (1 - \epsilon)\delta_{l,k} + \epsilon L$$

Feature extraction using VGG16

The 64 feature kernel filters constituting the first and second convolutional layers are of size 3x3. On moving through the first and second convolutional layers, the size of the input image is modified to 224x224x64 (depth 3 RGB image). This output is then passed to max pooling layer with a stride of 2. The 124 feature kernel filters of the third and fourth convolutional layers have filter size 3x3. Following these two is a max pooling layer with stride 2, the output will be decreased to 56x56x128. The fifth, sixth, and seventh convolutional layers have kernel dimensions 3x3. All three utilize 256 feature maps. They are followed by a stride 2 max pooling layer.

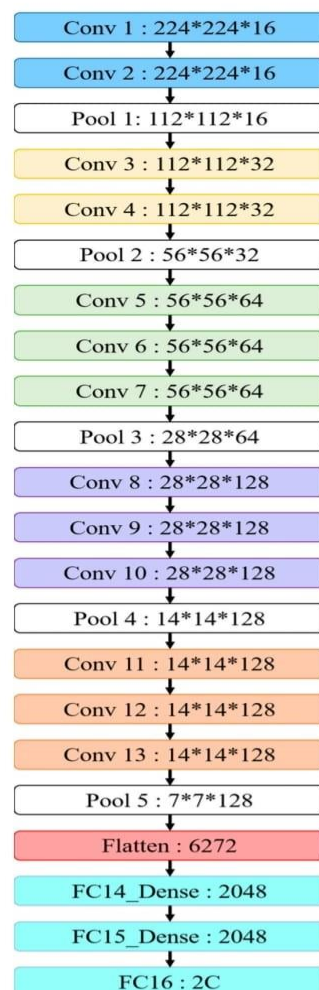


Figure 6: VGG16 Network Architecture

Feature Extraction using RESNET50

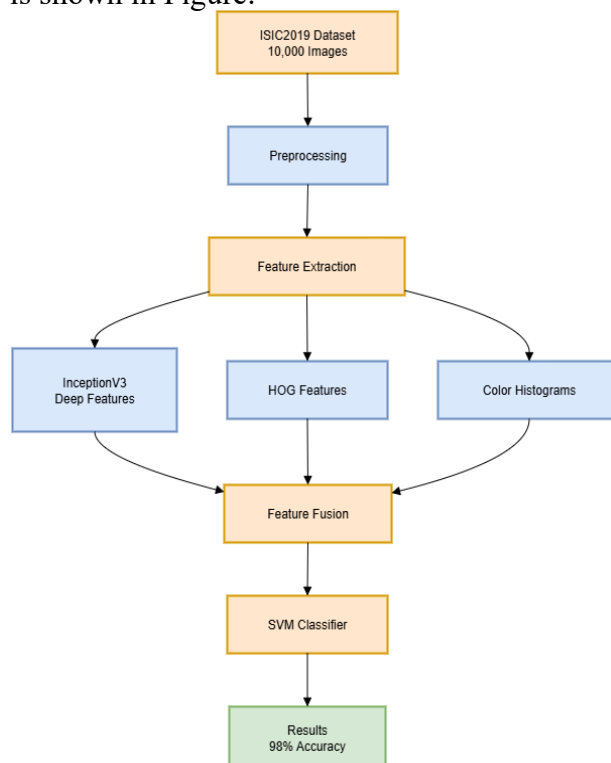
Since it can obtain higher precision and is easy to optimize, ResNet is regarded as a robust deep learning structure. Moreover, skip connections of the network are employed to solve the perpetual problem of vanishing gradients. With an increase in the layers of the deep network structure, the temporal complexity of the network also rises. This complexity can be avoided using a bottleneck architecture. Numerous models can be developed on top of ResNet-50. In image classification, a series of convolution networks known as ResNet-50 has shown superior performance. ResNet-50 is a 50-layer ResNet composed of 16 residual blocks, a layer of max-pooling, and a convolutional layer. Every residual block is made up of two 1×1 convolutional layers, a 3×3 convolutional layer, and skip connections from inputs to outputs. The feature width and height before putting the last fully linked layer are 32 times narrower and shorter compared to the original image width and height because ResNet-50 possesses a total stride of 32. (Elpeltagy & Sallam, 2021).

Proposed Methodology:

The proposed methodology is fusion of handcrafted feature with deep learning for efficient feature extraction in order to enhance image classification performance. The approach fuses the complementary strengths of manual handmade features and deep features from a pre-trained model named InceptionV3. Features are fused and classified using a support vector machine (SVM). The methodology has three primary stages:

1. Feature extraction,
2. Feature fusion,
3. Classification.

The pipeline overview is shown in Figure:



Feature extraction is carried out to yield deep as well as handcrafted representations of the input images, which capture different aspects of the data like texture, color, and high-level semantic information.

Deep Feature Extraction is carried out to get deep features, we use the InceptionV3, a previously trained model on dataset. The model is also applied as a feature extractor by stripping the top classification layer and using the global average pooling output, which generates a fixed-length feature vector for each input image. Preprocessing is applied to the input images to conform to the expected input dimensions of InceptionV3 (299×299 pixels) and normalize them with the standard preprocessing function for the model, scaling pixel values to the range $[-1, 1]$. For a collection of many images, each image is computed to produce a feature vector of size Ddeep (e.g., 2048 in InceptionV3). For computational efficiency, images are processed in batches, taking advantage of parallel computation features of contemporary hardware. Aside from deep features, two kinds of handcrafted features are computed to encode low-level image traits:

- **Histogram of Oriented Gradients (HOG):**

HOG features are calculated to describe local structures of gradients, which can well capture shape and edge information. For each image, the HOG descriptor is obtained as a Dhog-dimensional feature vector depending on the size of the image and HOG parameters

- **Color Histograms:**

Color histograms are utilized to define the boundaries between color intensities in the RGB channels. For every image, a histogram is calculated for every channel, and the concatenated histogram is a feature vector of size Dhist. This descriptor captures global color information, complemented by spatial information from HOG.

Feature Fusion: To integrate the merits of handcrafted and deep features, a feature fusion technique is utilized. For both training set and test set images, the deep features (Ddeep), HOG features (Dhog), and color histogram features (Dhist) are combined to create a fused vector of size.

$D_{fused} = D_{deep} + D_{hog} + D_{hist}$.

All the feature sets are normalized with z-score normalization, where every feature dimension has zero mean and unit variance, for compatibility with the SVM classifier. By preventing a particular feature type from dominating the process of categorization, this normalization reduces the impact of multi-scale heterogeneous features. The resulting fused feature matrices of the training and test sets are given as:

$X_{fused\ train} \in R^{N_{train} \times D_{fused}}$ and $X_{fused\ test} \in R^{N_{test} \times D_{fused}}$, respectively, where N_{train} and N_{test} are the number of train and test samples.

Classification

Training of a support vector machine (SVM) classifier with a linear kernel is done using the fused feature vectors. Due to its robustness in high-dimensional space and the ability to tackle multiclass classification with the one-vs-rest strategy, the SVM was chosen. By optimizing the hyperplane that optimizes the margin between classes, the classifier is trained on the combined training features $X_{fused\ train}$ and their corresponding labels y_{train} . In order to achieve a balance between generalization and model complexity, the regularization parameter C is tuned. Class labels of the test set $X_{fused\ test}$ are predicted using the SVM which has been trained. Based on a classification report, performance is also evaluated based on standard measures such as accuracy, precision, recall, and F1-score. To analyze performance per class and identify misclassifications, confusion matrix is also computed. TensorFlow for deep feature extraction, scikit-learn for SVM classification and feature pre-processing, and NumPy for numerical computation are the Python packages utilized to execute the methodology. By batch processing of images and GPU acceleration where applicable, the feature extraction process is optimized as much as possible.

All random operations (e.g. SVM initialization) are two seeded to ensure reproducibility, and feature preparation processes are run consistently across training and test sets in order to avoid data leaking.

Results and Discussion:

Table 2 presents performance measurements for a binary classifier model VGG16, which assesses two classes (Class 0 and Class 1) based on 517 examples. Some of these include precision, recall, F1-score, and support. The information reflects the model's performance with 117 samples upholding Class 0's precision at 0.99, recall at 0.77, and F1-score at 0.87. Class 1, on the other hand, shows a flawless recall rate of 1.00 at 400 samples, an F1-score of 0.97, and precision of 0.94. Overall accuracy is 0.95, with macro and weighted averages also showing the balanced and weighted performance of the model in both classes.

The performance metrics of classification (precision, recall, F1-score, and support) for the ResNet50 model applied to a two-class binary classification problem that was tested on a 517-sample dataset. Based on the results, Class 1 has 400 samples with precision, recall, and F1-score being 0.77, 1.00, and 0.87, respectively. The overall accuracy of the model is 0.77, the weighted averages of precision, recall, and F1-score are 0.60, 0.77, and 0.67, respectively, and the macro averages of precision, recall, and F1-score are 0.39, 0.50, and 0.44, respectively. These measures provide an overall evaluation of the classification performance of ResNet50 model and provide a good base for further analytical discussion.

After testing on a sample set of 517 samples with two classes (Class 0 and Class 1), the InceptionV3 model classification performance measures are presented in Table 1. The model, backed by 400 data, presents precision as 0.97, recall as 0.89, and F1-score as 0.93. For Class 0 for 117 instances, and accuracy of 0.97, recall of 0.99, and F1-score of 0.98 for Class 1. The likely overall accuracy of the model is 0.97. Also, the macro averages indicate a precision of 0.97, recall of 0.94, and an F1-score of 0.95, whereas the weighted averages indicate an accuracy, recall, and F1-score of 0.97, 0.97, and 0.97, respectively.

The classification performance metrics of the fusion model are presented in the next Table. The fusion was concatenation of handcrafted feature that is color histogram and deep model that is inceptionV3. Dataset is divided into two classes (Class 0, Class 1). The model has a precision of 0.97, recall of 0.89, and F1-score of 0.93 for Class 0, and a precision of 0.97, recall of 0.99, and F1-score of 0.98 for Class 1, supported by 400 samples. The overall accuracy of the model has been estimated to be 0.97. Also, the weighted averages have an accuracy of 0.97, recall of 0.97, and an F1-score of 0.97, while the macro averages have a precision of 0.97, recall of 0.94, and an F1-score of 0.95. Below is the table that illustrates comparison of performance of various models including CNN, Resnet50, VGG16, InceptionV3 and proposed fusion model.

| Model | Accuracy | Precision | Recall | F1 score |
|---|----------|-----------|--------|----------|
| CNN | 0.9284 | 0.9332 | 0.9775 | 0.9548 |
| Restnet50 | 0.7737 | 0.7737 | 1.0000 | 0.8724 |
| VGG16 | 0.9458 | 0.9366 | 0.9975 | 0.9661 |
| InceptionV3 | 0.5590 | 0.7671 | 0.6175 | 0.6842 |
| Proposed Model(InceptionV3+HOG+color hst+SVM) | 0.9845 | 0.9876 | 0.9925 | 0.9900 |

Table 2: Model Performance Comparison

The comparison of accuracy of some of the models like CNN, ResNet50, VGG16, InceptionV3, and a proposed model (InceptionV3 + HOG + ColorHist + SVM), which was

evaluated over a dataset, is presented in Figure 1. The accuracy of CNN is 0.93, while that of the ResNet50 is 0.77.

The accuracy of VGG16 is 0.95, whereas that of InceptionV3 is 0.56. More accurately at 0.98, the proposed model is superior to all others. This chart shows the higher accuracy of the proposed hybrid approach by providing a visual comparison of the relative performance of various models.

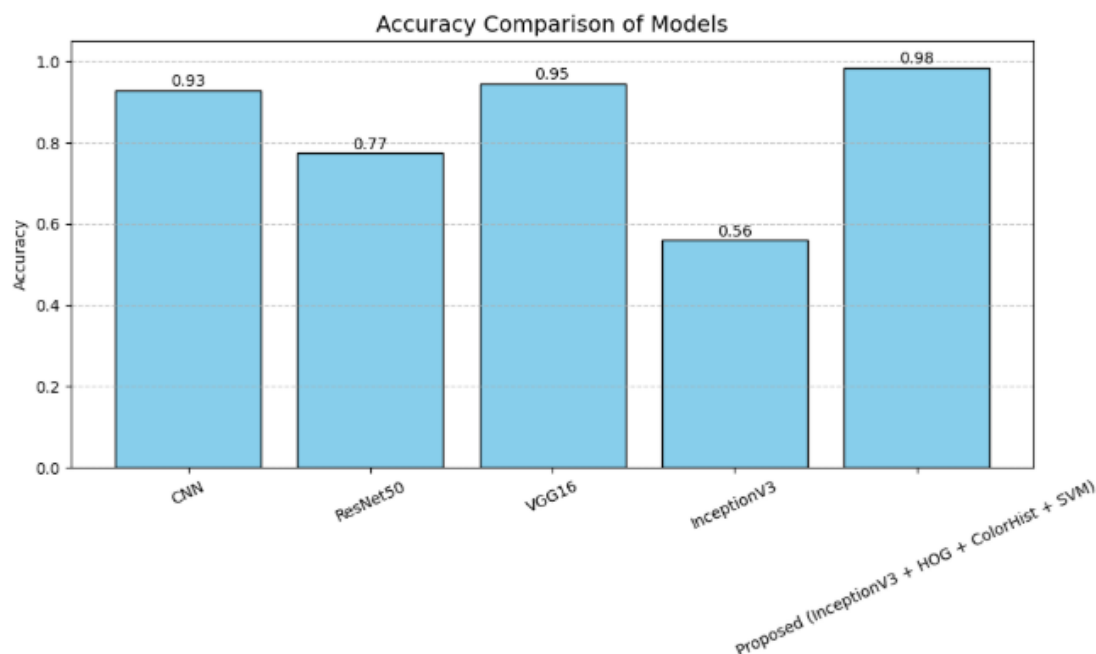


Figure 7: Accuracy Comparison of all models

Following figure displays Receiver Operating Characteristic (ROC) curve comparison of various models, i.e., CNN, ResNet50, VGG16, InceptionV3, and an enhanced model (InceptionV3 + HOG + SVM), tested on a dataset. The curves show the true positive rate vs. the false positive rate, and area under the curve (AUC) is used as model performance measure. The CNN model has an AUC of 0.982, ResNet50 has an AUC of 0.500, VGG16 has an AUC of 0.981, and InceptionV3 has an AUC of 0.481. The proposed model performs best with an AUC of 0.992, while the random classifier baseline is displayed with an AUC of 0.5. The graph provides a visualized comparison of the discriminative power of the models, highlighting the better performance of the proposed hybrid solution.

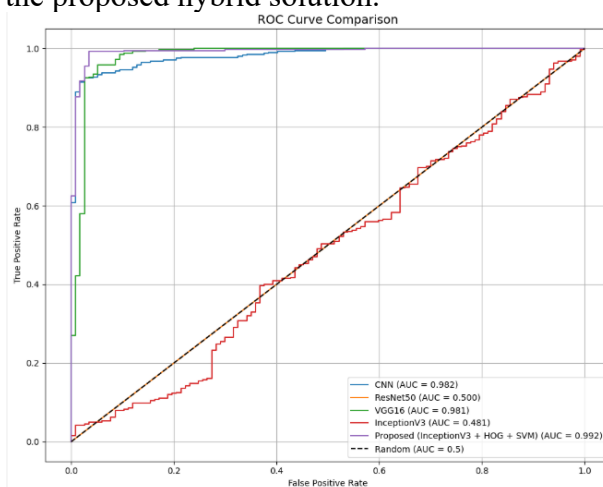


Figure 8: ROC Curve of all models

The training and validation loss patterns of the CNN model after eight epochs are illustrated in Figure 9, which indicates the process of learning of the model. The blue line indicates the loss in training, which begins at roughly 0.50 and decreases dramatically to roughly 0.20 by the second epoch before stabilizing with minor fluctuations between 0.15 and 0.20. An orange line indicates the validation loss, which starts at 0.50, drops in a similar manner initially to approximately 0.20, and then exhibits a sharp peak at the sixth epoch. Since the validation loss temporarily rises before dropping to around 0.15 by the seventh epoch, this peak opens the possibility of an overfitting issue. The graph shows how well the model can reduce training loss, but the validation loss spike suggests that more regularization is required.

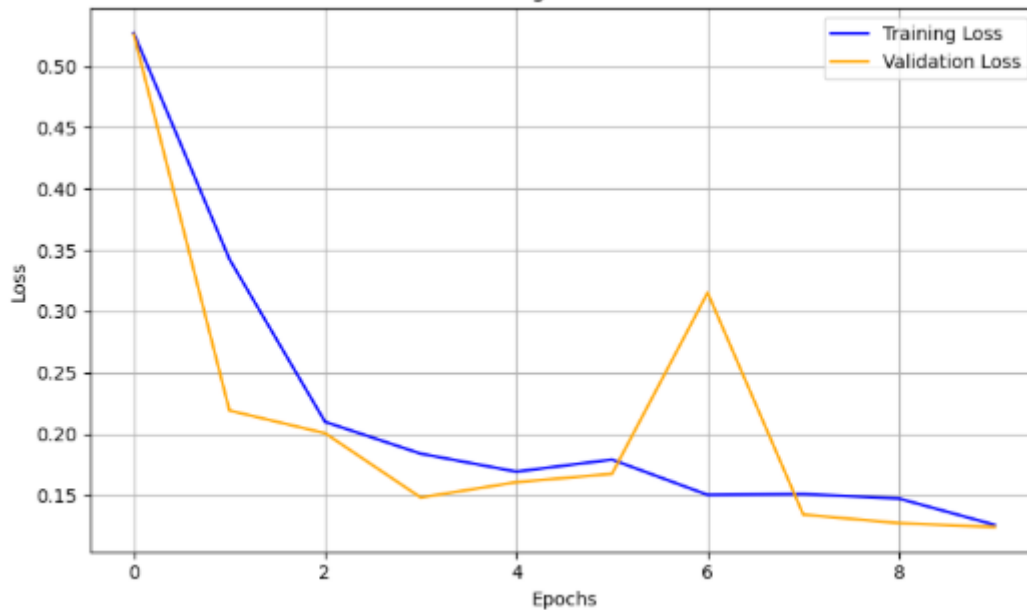


Figure 9: CNN Training and Validation Loss Curve

A thorough understanding of the ResNet50 model's training dynamics is provided by Figure 10, which shows the trends in training and validation loss over eight epochs. The blue line, the training loss, starts around 0.50 and quickly drops to around 0.20 by the second epoch and stays constant with very small fluctuations between 0.15 and 0.20. The orange-colored validation loss begins at 0.50, falls to around 0.20 by the second epoch, and then increases significantly around the sixth epoch. This peak in validation loss, which rises briefly before diminishing to roughly 0.15 by the seventh epoch, indicates a possible case of overfitting. Unlike the fluctuation of validation loss, however, the drop in training loss is steady, indicating that the model generalizes effectively outside the initial epochs.

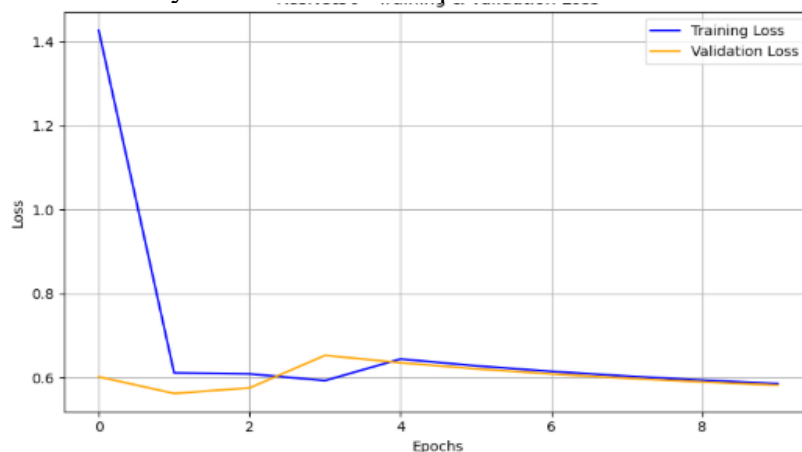


Figure 10: Resnet50 Training and Validation Loss Curve

Patterns in the training and validation loss of the VGG16 model over eight epochs are presented here, providing a comprehensive picture of learning. A blue line indicates the loss during training, which starts at around 0.50 and approaches almost vertically to around 0.20 by the second epoch before flattening with small fluctuations between 0.15 and 0.20. An orange line indicates the validation loss, which initiates at 0.50, reduces in the same way to around 0.20, and then spikes evidently around the sixth epoch. The validation loss temporarily rose before stabilizing at about 0.15 by epoch seven, signaling the potential presence of an overfitting issue. The plot indicates the extent to which the VGG16 model minimizes training loss, but the spike in validation loss highlights the necessity for techniques to enhance generalization.

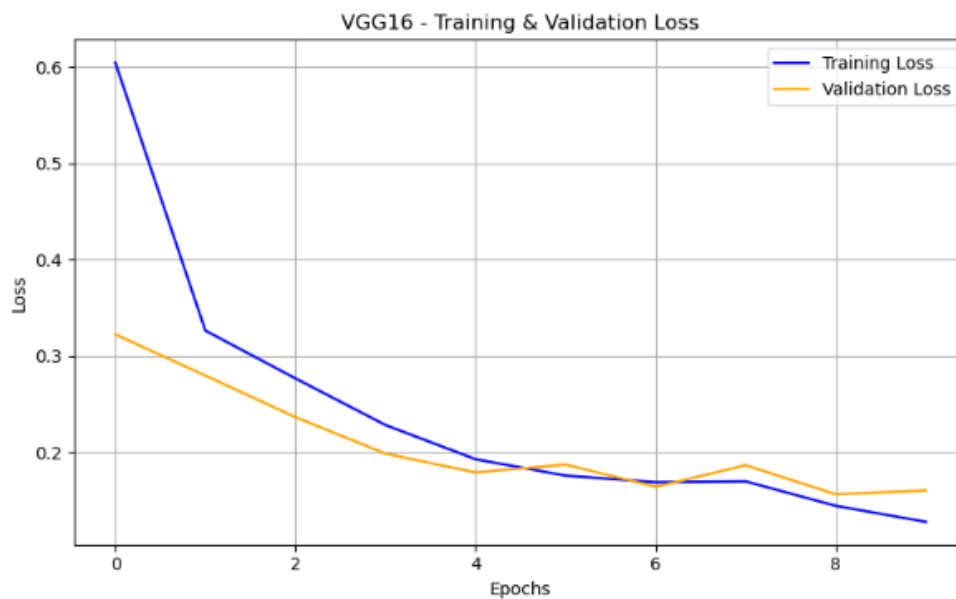


Figure 11: VGG16 Training and Validation Loss Curve

The training progression of the InceptionV3 model is unveiled by Figure 12, showing the training and validation loss patterns over eight epochs. A blue line tracks the training loss, which starts at roughly 1.40 and drops precipitously to roughly 0.10 by the second epoch and then remains largely steady with little variation. The orange-hued validation loss begins at roughly 0.60, declines to roughly 0.10 by the second epoch, and then continues trending steadily with hardly any variation, remaining close to the training loss. InceptionV3 performs better overall across epochs compared to the other models, as indicated by the absence of a sharp validation loss peak. The steady performance indicates that the model learns and adapts to the data without being overfit.

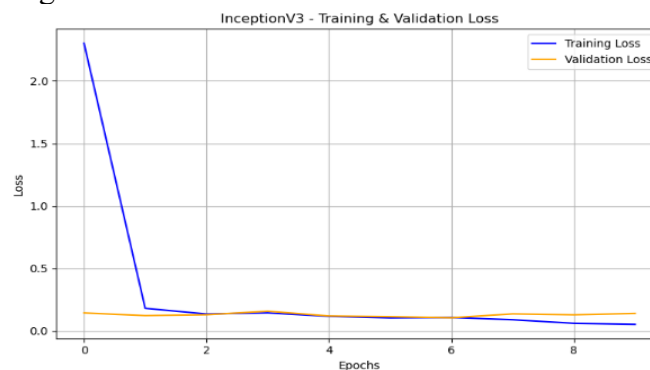


Figure 12: InceptionV3-Training&Validation Loss

Conclusion:

This paper blends manual features with deep learning to present a good and interpretable approach to melanoma diagnosis. Both high-level and low-level image features are captured through the proposed hybrid model by applying InceptionV3 to learn deep semantic features and augmenting it with manually designed descriptors like HOG and Color Histograms. When a Support Vector Machine classifier is applied to the resultant fused feature set, it classifies better across a range of evaluation metrics compared to single deep learning models. Interestingly, the proposed model performed better than such state-of-the-art CNN models as VGG16 and ResNet50, with a correctness rate of 98%. The findings corroborate the hypothesis that discriminative ability and stability of the model are enhanced by blending deep and manual features. The system can potentially be applied to clinical diagnosis, as seen with its reliable performance across diverse skin lesion types. In order to enhance the utility and accessibility of the model in resource-limited environments, future studies may consider incorporating metadata and real-time deployment in mobile dermoscopy software.

References:

- Zainab, H., Khan, A. R. A., Khan, M. I., & Arif, A. (2025). Ethical Considerations and Data Privacy Challenges in AI-Powered Healthcare Solutions for Cancer and Cardiovascular Diseases. *Global Trends in Science and Technology*, 1(1), 63-74.
- Sardar, M., Niazi, M. M., & Nasim, F. (2024). Ensemble deep learning methods for detecting skin cancer. *Bulletin of Business and Economics (BBE)*, 13(1).
- Nasim, M. F., & Ahmad, J. (2025). Optimizing the Efficacy of Bagging Ensemble Deep Learning Models in Melanoma Skin Cancer Diagnosis. *Journal of Innovative Computing and Emerging Technologies*, 5(1).
- Zainab, H., Khan, A. R. A., Khan, M. I., & Arif, A. (2025). Innovative AI Solutions for Mental Health: Bridging Detection and Therapy. *Global Journal of Emerging AI and Computing*, 1(1), 51-58.
- Asim, M., Nasim, F., Sehar, H., & Naseem, S. (2025). A DEEP LEARNING-BASED APPROACH FOR HEART DISEASE DETECTION AND EARLY WARNING. *Contemporary Journal of Social Science Review*, 3(2), 2856-2872.
- Khan, A. R. A., Khan, M. I., & Arif, A. (2025). AI in Surgical Robotics: Advancing Precision and Minimizing Human Error. *Global Journal of Computer Sciences and Artificial Intelligence*, 1(1), 17-30.
- Nasim MF, Anwar M, Alorfi AS, Ibrahim HA, Ahmed A, Jaffar A, Akram S, Siddique A, and Zeeshan HM (2025). Cognitively inspired sound-based automobile problem detection: A step toward explainable AI (XAI). *International Journal of Advanced and Applied Sciences*, 12(8): 1-15
- Zainab, H., Khan, M. I., Arif, A., & Khan, A. R. A. (2025). Development of Hybrid AI Models for Real-Time Cancer Diagnostics Using Multi-Modality Imaging (CT, MRI, PET). *Global Journal of Machine Learning and Computing*, 1(1), 66-75.
- Nasim, F., Masood, S., Jaffar, A., Ahmad, U., & Rashid, M. (2023). Intelligent Sound-Based Early Fault Detection System for Vehicles. *Computer Systems Science & Engineering*, 46(3).
- Khan, M. I. Synergizing AI-Driven Insights, Cybersecurity, and Thermal Management: A Holistic Framework for Advancing Healthcare, Risk Mitigation, and Industrial Performance. *Global Journal of Computer Sciences and Artificial Intelligence*, 1(2), 40-60.
- Zainab, H., Khan, M. I., Arif, A., & Khan, A. R. A. (2025). Deep Learning in Precision Nutrition: Tailoring Diet Plans Based on Genetic and Microbiome Data. *Global Journal of Computer Sciences and Artificial Intelligence*, 1(1), 31-42.
- Khan, A. R. A., Khan, M. I., Arif, A., Anjum, N., & Arif, H. (2025). Intelligent Defense: Redefining OS Security with AI. *International Journal of Innovative Research in Computer Science and Technology*, 13, 85-90.
- Shamshirband, S., Fathi, M., Dehzangi, A., Chronopoulos, A. T., & Alinejad-Rokny, H. (2021). A review on deep learning approaches in healthcare systems: Taxonomies, challenges, and open issues. *Journal of Biomedical Informatics*, 113, 103627.

- Khan, M. I., Arif, A., & Khan, A. R. A. (2024). The Most Recent Advances and Uses of AI in Cybersecurity. *BULLET: Jurnal Multidisiplin Ilmu*, 3(4), 566-578.
- Arif, A., A. Khan, and M. I. Khan. "Role of AI in Predicting and Mitigating Threats: A Comprehensive Review." *JURIHUM: Jurnal Inovasi dan Humaniora* 2, no. 3 (2024): 297-311.
- Tariq, Muhammad Arham, Muhammad Ismaeel Khan, Aftab Arif, Muhammad Aksam Iftikhar, and Ali Raza A. Khan. "Malware Images Visualization and Classification With Parameter Tunned Deep Learning Model." *Metallurgical and Materials Engineering* 31, no. 2 (2025): 68-73. <https://doi.org/10.63278/1336>.
- Zainab, H., Khan, A., Raza, A., Khan, M. I., & Arif, A. (2025). Integration of AI in Medical Imaging: Enhancing Diagnostic Accuracy and Workflow Efficiency. *Global Insights in Artificial Intelligence and Computing*, 1(1), 1-14.
- Arif, A., Shah, F., Khan, M. I., Khan, A. R. A., Tabasam, A. H., & Latif, A. (2023). Anomaly detection in IoHT using deep learning: Enhancing wearable medical device security. *Migration Letters*, 20(S12), 1992–2006.
- Khan, M. I., Arif, A., Khan, A. R. A., Anjum, N., & Arif, H. (2025). The Dual Role of Artificial Intelligence in Cybersecurity: Enhancing Defense and Navigating Challenges. *International Journal of Innovative Research in Computer Science and Technology*, 13, 62-67.
- Khan, M. I., Arif, A., & Khan, A. R. A. (2024). AI's Revolutionary Role in Cyber Defense and Social Engineering. *International Journal of Multidisciplinary Sciences and Arts*, 3(4), 57-66.
- Tselios, D. (2022). Combining deep learning, handcrafted features, and metadata for the classification of dermoscopy images.
- Jojoa Acosta, M. F., Caballero Tovar, L. Y., Garcia-Zapirain, M. B., & Percybrooks, W. S. (2021). Melanoma diagnosis using deep learning techniques on dermatoscopic images. *BMC Medical Imaging*, 21, 1–11.
- Jain, S., & Pise, N. (2015). Computer aided melanoma skin cancer detection using image processing. *Procedia Computer Science*, 48, 735–740.
- Arif, A., Khan, M. I., & Khan, A. R. A. (2024). An overview of cyber threats generated by AI. *International Journal of Multidisciplinary Sciences and Arts*, 3(4), 67-76.
- Khan, M. I., Arif, A., & Khan, A. R. A. (2024). AI-Driven Threat Detection: A Brief Overview of AI Techniques in Cybersecurity. *BIN: Bulletin of Informatics*, 2(2), 248-61.
- Rejeesh, M. (2019). Interest point based face recognition using adaptive neuro fuzzy inference system. *Multimedia Tools and Applications*, 78(16), 22691–22710.
- Adegun, A. A., & Viriri, S. (2019). Deep learning-based system for automatic melanoma detection. *IEEE Access*, 8, 7160–7172.
- Almaraz-Damian, J.-A., Ponomaryov, V., Sadovnychiy, S., & Castillejos-Fernandez, H. (2020). Melanoma and Nevus Skin Lesion Classification Using Handcraft and Deep Learning Feature Fusion via Mutual Information Measures. *Entropy*, 22(4), 484. <https://doi.org/10.3390/e22040484>
- Bansal, P., Garg, R., & Soni, P. (2022). Detection of melanoma in dermoscopic images by integrating features extracted using handcrafted and deep learning models. *Computers & Industrial Engineering*, 168, 108060.
- Chaturvedi, S. S., Tembhurne, J. V., & Diwan, T. (2020). A multi-class skin Cancer classification using deep convolutional neural networks. *Multimedia Tools and Applications*, 79(39), 28477–28498.
- Codella, N., Rotemberg, V., Tschandl, P., Celebi, M. E., Dusza, S., Gutman, D., Helba, B., Kalloo, A., Liopyris, K., & Marchetti, M. (2019). Skin lesion analysis toward melanoma detection 2018: A challenge hosted by the international skin imaging collaboration (isic). *arXiv Preprint arXiv:1902.03368*.
- Elpeltagy, M., & Sallam, H. (2021). Automatic prediction of COVID- 19 from chest images using modified ResNet50. *Multimedia Tools and Applications*, 80(17), 26451–26463.
- Esteva, A., Kuprel, B., Novoa, R. A., Ko, J., Swetter, S. M., Blau, H. M., & Thrun, S. (2017). Dermatologist-level classification of skin cancer with deep neural networks. *Nature*, 542(7639), 115–118.

- Filali, Y., EL Khoukhi, H., Sabri, M. A., & Aarab, A. (2020). Efficient fusion of handcrafted and pre-trained CNNs features to classify melanoma skin cancer. *Multimedia Tools and Applications*, 79(41), 31219–31238.
- Hagerty, J. R., Stanley, R. J., Almubarak, H. A., Lama, N., Kasmi, R., Guo, P., Drugge, R. J., Rabinovitz, H. S., Oliviero, M., & Stoecker, W. V. (2019). Deep learning and handcrafted method fusion: Higher diagnostic accuracy for melanoma dermoscopy images. *IEEE Journal of Biomedical and Health Informatics*, 23(4), 1385–1391.
- Hidaka, A., & Kurita, T. (2017). Consecutive dimensionality reduction by canonical correlation analysis for visualization of convolutional neural networks. 2017, 160–167.
- Jayapriya, K., & Jacob, I. J. (2020). Hybrid fully convolutional networks-based skin lesion segmentation and melanoma detection using deep feature. *International Journal of Imaging Systems and Technology*, 30(2), 348–357.
- Khan, M. S. I., Rahman, A., Debnath, T., Karim, M. R., Nasir, M. K., Band, S. S., Mosavi, A., & Dehzangi, I. (2022). Accurate brain tumor detection using deep convolutional neural network. *Computational and Structural Biotechnology Journal*, 20, 4733–4745.
- LeCun, Y., Haffner, P., Bottou, L., Bengio, Y., Bottou, L., Haffner, P., Howard, P., Simard, P., Bengio, Y., & LeCun, Y. (1988). Object recognition with gradient-based learning. *Feature Grouping*, 66, 233–240.
- Mahum, R., & Aladhadh, S. (2022). Skin lesion detection using hand-crafted and DL-based features fusion and LSTM. *Diagnostics*, 12(12), 2974.
- Majtner, T., Yildirim-Yayilgan, S., & Hardeberg, J. Y. (2016). Combining deep learning and hand-crafted features for skin lesion classification. 1–6.
- Mishra, N. K., & Celebi, M. E. (2016). An overview of melanoma detection in dermoscopy images using image processing and machine learning. *arXiv Preprint arXiv:1601.07843*.
- Mohammed, M. G., & Melhum, A. I. (2020). Implementation of HOG feature extraction with tuned parameters for human face detection. *International Journal of Machine Learning and Computing*, 10(5), 654–661.
- Muhamad Yani, S. (2019). Application of Transfer Learning Using Convolutional Neural Network Method for Early Detection of Terry's Nail. 1201(1), 012052.
- Pathan, S., Prabhu, K. G., & Siddalingaswamy, P. (2018). Techniques and algorithms for computer aided diagnosis of pigmented skin lesions—A review. *Biomedical Signal Processing and Control*, 39, 237–262.
- Rahman, M. M., Nasir, M. K., Nur, A., Khan, S. I., Band, S., Dehzangi, I., Beheshti, A., & Rokny, H. A. (2022). Hybrid feature fusion and machine learning approaches for melanoma skin cancer detection.